

**Title** A Steady-State Simulation Tool for MCFC Systems Suitable for On-line Applications

**Authors** Paolo Greppi, Barbara Bosio\*, Elisabetta Arato

**Affiliation** DICAT, University of Genova, Via Opera Pia 15, 16145 Genova, Italy

Accepted for publication in International Journal of Hydrogen Energy (ISSN: 0360-3199), July 07, 2008.

### Abstract

The steady-state model of a Molten Carbonate Fuel Cell (MCFC) energy plant can be formulated with differing degrees of detail and implemented within any of the frameworks available today, but it is difficult to obtain an efficient, lean, robust simulation tool also capable of providing sensitivities. If such a tool were available, there would be much to gain in applying it on-line to support the operation of these plants.

In this paper we present a new system simulation tool for MCFC energy plants, based on a simplified model and implemented with the general purpose C++ process simulation library LIBPF. We have tested our approach for an application example based on a reference hybrid 1 MW<sub>el</sub> MCFC-gas turbine energy plant. With the new tool it proved possible to analyse off-line the degrees of freedom when all operational constraints are considered, and to study the system part-load behaviour. The tool is also suitable for integration in an on-line application.

**Keywords** Fuel cell system, Flowsheeting, Sensitivity, Modelling

### Nomenclature

A	area, m <sup>2</sup>
C <sub>p</sub>	specific heat, J/mol K
F	Faraday's constant, C/mol
G	Gibbs' free energy, J/mol
H	enthalpy, J/mol
J	current density, A/m <sup>2</sup>
k	empirical coefficients for the pressure drop correlation (flow coefficient), kg/m <sup>7</sup>
K	equilibrium constant
l	length of the rectangular active area of each planar fuel cell perpendicular to the cathodic inlet, m
LHV	Lower Heating Value, J/kg
$\dot{m}$	mass flow, kg/s
n	compressor rotational frequency, Hz
$\dot{n}$	mole flow, kmol/s
N	number of fuel cells in the stack
P	pressure, Pa
R	gas constant, J/mol K
T	temperature, K
U	heat transfer coefficient, W/m <sup>2</sup> /K
v	volume flow, m <sup>3</sup> /s
V	voltage, V
w	width of the rectangular active area of each planar fuel cell along the cathodic inlet, m
W	power, W
x	molar fractions
$\bar{x}$	vector of input variables
$\bar{y}$	vector of output variables
z	number of charges in the electrochemical reaction

Greek letters:

$\beta$  compressor pressure ratio

---

\* Corresponding author; Fax: +39 010 3532589; e-mail: barbara.bosio@unige.it

$\theta$	isentropic efficiency
$\eta$	efficiency
$\nu$	stoichiometric coefficient
$\Delta$	variation

Subscripts:

an	anode
avg	average
cat	cathode
co	cold side
CV	controlled variables
el	electrical
f	fluid
FF	feed-forward variables
ho	hot side
i	component index
in	inlet
me	mechanical, shaft
MV	manipulated variables
OC	open circuit
offset	offset empirical correction parameter, added to the intermediate fidelity to match the rigorous model results
out	outlet
r	reaction
th	thermal
$\theta$	thermodynamic

Superscripts:

'	corrected
0	reference state, nominal point
is	isentropic
nom	nominal

## 1. Introduction

Fuel Cells can efficiently convert hydrogen into electrical energy; in particular high-temperature fuel cells can be fed with hydrogen-rich gas and provide high-level thermal energy suitable for sustaining the reforming of hydrocarbon fuels, producing pressurised steam and finally cogeneration.

Today Molten Carbonate Fuel Cells (MCFCs) are closer to commercial release than any other high-temperature fuel cell type and look promising for implementing clean, distributed Combined Heat and Power (CHP). This is reflected in the medium-term quantitative target of Innovation and Development Actions 3 "Competitive Fuel Cells for CHP and Power Generation" of the European HFP Advisory Council [1] which involves installing at least "2600 10 kW - 1 MW units in industrial use and a further 50 units of 1 MW or more also in industrial use".

In the distributed CHP scenario MCFC energy plants with nominal electrical output in the range 200-2000 kW<sub>el</sub> would be packaged as stand-alone units and deployed in remote locations where they would function in the absence of any plant operator.

From the point of view of control a steady-state MCFC energy plant can be considered as a black box with a few Controlled output Variables (CVs, such as maximum temperature in the fuel cell plane, cathodic inlet oxygen and carbon dioxide molar concentrations, net power production, etc.), a few Feed-Forward input Variables (FFs, such as fuel composition when the fuel is derived from a biomass source or a variable mixture of biomass-derived syngas, day-night ambient temperature fluctuation, deterioration in the performance the reformer catalyst, fouling of the heat exchangers or ageing of the cells) and a few Manipulated input Variables (MVs, discussed below).

The basic control problem can be stated as a servo problem (the objective is to produce the

required electrical power and/or thermal duty) subject to feed-forward perturbations and to a number of algebraic inequality constraints expressed in terms of the controlled variables:

$$\text{Implicit model formulation:} \quad f(\bar{y}_{CV}, \bar{x}_{MV}, \bar{x}_{FF}) = 0 \quad (1)$$

$$\text{Required loads:} \quad g(\bar{y}_{CV}) = 0 \quad (2)$$

$$\text{Algebraic inequality constraints:} \quad h(\bar{y}_{CV}) < 0 \quad (3)$$

The challenge is to obtain safe and economically optimal operation, but also flexibility: changes in electrical or thermal load of 30-110% with respect to the nominal are to be expected in real-world applications. While the fuel cell itself can produce energy with an optimal efficiency over a broad operating range (flat efficiency/load curve), it is necessary to make this true for the system as a whole.

The application of identification, data reconciliation, advanced process control and non-linear model predictive control techniques to this plant is very interesting; given the high thermal inertia and slow time constant, initially even applying steady-state models can bring benefits. But this kind of application requires a steady-state system simulation tool suitable for forming the core model of an on-line application, i.e.:

- capable of providing first-order analytical derivatives (sensitivities);
- efficient, i.e. fast;
- accurate to a sufficient degree;
- robust;
- lean and lightweight.

The last requirement, in particular, derives from the tight economic constraint on the cost of an MCFC energy plant and therefore on the control system which includes the model.

The capital cost of conventional 800 MW<sub>el</sub> combined-cycle natural-gas-fed power stations is in the range of about 500 €/kW<sub>el</sub> installed [2], while the cost of CHP plants based on internal combustion engines in the 500 kW<sub>el</sub> range is about 1000 €/kW<sub>el</sub> installed. The target system-cost for stationary applications with power higher than 100 kW<sub>el</sub> in the time frame 2009 - 2012 according to [1] is 1500 - 5000 €/kW<sub>el</sub> installed.

So when the technology is mature, a realistic 1 MW<sub>el</sub> MCFC energy plant will have a budget in the order of magnitude of 1 M€, and the impact of the control system on the capital cost must be limited.

As a consequence the process model should strike a compromise between accuracy and complexity. For its implementation it is clearly not feasible to employ an integrated modelling environment which would not run on the low-cost embedded hardware likely to be used as control system for these plants. It is also not feasible to use a modelling system conceived for reconciliation or Real-Time Optimization (RTO) in the petrochemicals industry or in the traditional, centralized power sector. Finally 3-D distributed parameters models with thousands of variables are too slow and lack the necessary robustness, while concentrated parameter models for certain units (fuel cell, planar reactive heat exchanger) lack key information.

In this paper we will:

- formulate an intermediate-fidelity system model (see definition at section “Fuel Cell Sub-system Modelling”) for a reference hybrid 1 MW<sub>el</sub> MCFC-gas turbine energy plant;
- implement the model using the general purpose process flowsheeting library LIBPF, producing a robust, lightweight, flexible simulation tool;
- tune and validate the tool against a rigorous reference model, also setting up a method to exactly match the results of the reference model, at least in the vicinity of a certain operating point;
- test off-line the approach for the reference plant, using the tool to study the operating constraints and degrees of freedom and to analyze the part-load behaviour with sensitivity studies.

## 2. Process Description

The reference 1 MW<sub>el</sub> MCFC energy plant is a hybrid MCFC-gas turbine system already presented in a previous publication of one of the authors [3]; its process scheme is shown in Figure 1.

The Fuel-Cell Sub-system (FCS) consists of four separate pressure vessels for the planar, rectangular, and cross-flow stacks together with the common Balance of Plant (BoP) which is placed outside the vessels: the external reformer, catalytic burner (R1), pre-heater (REGHEX) and recycle blower. The Gas Turbine Sub-system (GTS) is a recuperated-gas turbine-driven air-compressor complete with a separate burner (R2). The turbine exhaust from the GTS proceeds to the Steam Production Sub-system (SPS) and finally to the cogenerative heat exchanger (COGEN). The main operating parameters at the nominal point are shown in Table 1.

The plant electrical efficiency is defined as the net electrical power produced, divided by the maximum power that can be obtained from the fuel to FCS and to GT, expressed in terms of Lower Heating Value (LHV); the net electrical power in turn is computed as the electrical output from the stack and turbine minus the compressor and blower power consumptions:

$$W_{el,net} = W_{el,FC} + W_{el,T} - W_{el,C} - W_{el,BLOWER} \quad (4)$$

$$\eta_{el} = \frac{W_{el,net}}{LHV \cdot (m_{fuel,FCS} + m_{fuel,GTS})} \quad (5)$$

Although the raw MCFC power output is direct current (DC), and an inverter would be required to convert it to alternate current (AC) for utilization, the inverter energy loss was neglected; the impact on the electrical power of such accessories as the control system, the feed water pump and the fuel booster compressor has been neglected too.

### 3. Formulation and Implementation of the Model

From the point of view of modelling complexity, the simulation of MCFC energy plant systems is not a challenging task. The components present are selected from a list of a dozen chemical species; the operating pressure is moderate, allowing the use of the perfect-gas and ideal-mixture approximations; chemical equilibrium or complete conversion in the reactors can safely be assumed; phase equilibriums are not relevant and the choice of unit operations employed is limited.

The complexity arises from the hybrid unit operations such as the MCFC stack and the reactive heat exchanger where the reforming takes place, which are intrinsically distributed. The distributed-parameter approach for these hybrid units provides an insight into the local values of the variables. Only with this insight, is it possible to operate in a safe and optimal way; in particular one of the most important constraints on the operation of MCFC energy plants is the maximum temperature inside the stack plane.

In the present work the following seven chemical species were considered: water (H<sub>2</sub>O), nitrogen (N<sub>2</sub>), oxygen (O<sub>2</sub>), methane (CH<sub>4</sub>), carbon monoxide (CO), carbon dioxide (CO<sub>2</sub>) and hydrogen (H<sub>2</sub>).

All materials were considered in the gas phase, except for the water feed to the SPS which was considered in the liquid phase.

The reference state for the thermodynamic computations was the pure component in the perfect gas phase, P<sup>0</sup>=101.325 kPa and T<sup>0</sup>= 298 K.

Gas mixtures were treated as ideal mixtures of perfect gases, therefore the mixture enthalpy and Gibbs free energy could be computed as the mole-average of the corresponding pure components property. The pure components enthalpy and Gibbs free energy were computed from the property at the reference state and the integral of the perfect gas specific heats using the expressions:

$$H_i(T) = \Delta H_i^0 + \int_{T^0}^T C_{p,i}(T) \cdot dt \quad (6)$$

$$G_i(T) = \Delta G_i^0 + \int_{T^0}^T C_{p,i}(T) \cdot dt - T \cdot \left( \int_{T^0}^T \frac{C_{p,i}(T)}{T} \cdot dt - R \cdot \ln \left( \frac{P}{P^0} \right) \right) \quad (7)$$

where the integrals are computed analytically.

The pure components enthalpy and Gibbs free energy at the reference state, from [4] are shown in Table 2.

The correlations and coefficients for the perfect gas specific heats were those of [5] for all species except water; for water the correlations and coefficients from [6] were used.

All feeds enter at ambient temperature. The fuels and feed water enter the system already at the system pressure, while ambient air enters at 101.325 kPa absolute pressure.

Ambient air humidity is neglected, and the N<sub>2</sub>/O<sub>2</sub> composition of the air was 21%/79% by moles.

The fuel feeds to the FCS and to the GTS were both natural gas, approximated as pure methane.

The feed to SPS was considered to be pure water.

Unit operation modelling is generally based on mass- and energy-balances and the assumption of adiabatic operation; in the following the specific modelling features are highlighted.

The heat exchangers are simulated using the well-known expressions:

$$\left\{ \begin{array}{l} Q = (U \cdot A) \cdot \Delta T_{LM} \\ \Delta T_{LM} = \frac{(\Delta T_{out} - \Delta T_{in})}{\ln \left( \frac{\Delta T_{out}}{\Delta T_{in}} \right)} \\ \Delta T_{in} = T_{in,ho} - T_{out,co} \\ \Delta T_{out} = T_{out,ho} - T_{in,co} \end{array} \right. \quad (8)$$

with the numerical values for the empirical (U·A) parameters being fixed by matching the temperature approaches found in industrial practice.

Only for the heat exchange in the COGEN system a constant-temperature was set for the process side (flue gas) since the hot water circuit is outside our scope.

The cathode gas recirculation blower and the compressor / expander in the GT were modelled as based on isentropic expansions/compressions with an applied isentropic efficiency; the equations for the compressor and the blower are:

$$\left\{ \begin{array}{l} W_f = \frac{W_f^{is}}{\theta} \\ W_{me} = \frac{W_f}{\eta_{me}} \\ W_{el} = \frac{W_{me}}{\eta_{el}} \end{array} \right. \quad (9)$$

whereas for the expander they are:

$$\left\{ \begin{array}{l} W_f = W_f^{is} \cdot \theta \\ W_{me} = W_{is} \cdot \eta_{me} \\ W_{el} = W_{me} \cdot \eta_{el} \end{array} \right. \quad (10)$$

The reactions in the reformer were assumed at chemical equilibrium; the significant reactions that occur at the conditions of interest between the chemical species present (the controlling equilibria) are:

Reforming of methane:  $\text{CH}_4 + \text{H}_2\text{O} \leftrightarrow \text{CO} + 3\cdot\text{H}_2$ ,  $\Delta H_r^0 = 205.804 \text{ kJ/mol}$

Water gas shift:  $\text{CO} + \text{H}_2\text{O} \leftrightarrow \text{CO}_2 + \text{H}_2$ ,  $\Delta H_r^0 = -41.166 \text{ kJ/mol}$

All reaction equilibria are computed solving the algebraic formulation:

$$K_{eq} = \prod \left( \frac{P_i}{P^0} \right)^{v_i} \quad (11)$$

where the equilibrium constant  $K_{eq}$  is computed from the Gibbs free energy change of the reaction based on the expression:

$$\ln(K_{eq}) = -\frac{\Delta G_r(T, P)}{R \cdot T} \quad (12)$$

The Gibbs' free energy change of the reaction is computed from the individual components Gibbs free energy at the reaction conditions weighted by the stoichiometric coefficients:

$$\Delta G_r(T, P) = \sum (G_i(T, P) \cdot v_i) \quad (13)$$

In the catalytic combustor and in the turbine burner the complete, adiabatic combustion of methane, hydrogen and carbon monoxide to water and carbon dioxide is assumed.

The thermal losses from units inside the vessel towards the ambient have been neglected.

The pressure drops in the REFORMER cold side and in both sides of the REGHEX were neglected; the pressure drops of the REFORMER hot side and of both sides of the RECUPERATOR were set at the nominal point, but when simulating operating points away from the nominal, the effect of changing flows upon some of these pressure drops was accounted for using the empirical expression:

$$\Delta P = k \cdot v^2 \quad (14)$$

### 3.1 Fuel Cell Sub-system Modelling

In the preceding publication [3], a detailed rigorous approach for the steady-state modelling of the FCS is used, with distributed-parameter models for the fuel cell (2-D, adiabatic) and for the reformer (1-D).

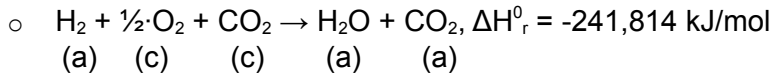
For the sake of reducing the complexity of the model and the associated computational cost, the modelling of the Fuel-Cell Sub-system was simplified for this work; however all the information on the maximum temperature in the fuel cell plane would be lost if the MCFC stack were to be modelled with a straight concentrated-parameter approach. Our goal was to retain a distributed-parameter model for this unit, albeit with a very coarse discretisation. The intermediate fidelity model for the FCS is therefore characterised by the two following simplifications:

- a concentrated parameter reactive heat-exchanger was set up in place of the series (about a dozen) of heat exchangers and concentrated parameter reforming reactor pairs used in the reference;
- a very coarse discretisation of 3 units along the direction perpendicular to the cathode flow, and of 2 units along the orthogonal direction was used for the planar, rectangular fuel cell in place of the 24x16 discretisation used in the reference.

In particular the behaviour for each of the discretized sub-fuel cells was calculated with the following specific assumptions:

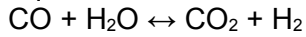
- The electrochemical reaction is:
  - cathode:  $\frac{1}{2} \cdot \text{O}_2 + \text{CO}_2 + 2 \cdot \text{e}^- \rightarrow \text{CO}_3^{--}$
  - anode:  $\text{H}_2 + \text{CO}_3^{--} \rightarrow \text{H}_2\text{O} + \text{CO}_2 + 2 \cdot \text{e}^-$

resulting in the overall reaction:



where the letters underneath indicate anode compartment (a) and cathode compartment (c);

- gas cross-over neglected;
- diffusion effects neglected;
- the FC anode and cathode side pressure-drops were fixed;
- thermal diffusion in the solid neglected;
- water gas shift reaction in the anode compartment is assumed to be at thermodynamic equilibrium:



(a) (a) (a) (a)

- no reforming reaction takes place.

The thermodynamic voltage is computed from the Gibbs' free energy change of the reaction (13):

$$V_\theta = \frac{\Delta G_r(T, P)}{z \cdot F} \quad (15)$$

The Open Circuit Voltage (OCV) is computed based on an arithmetic mean between inlet and outlet equilibrium constants of each discretized cell:

$$V_{OC} = V_\theta + \frac{R \cdot T}{z \cdot F} \cdot \ln(K_{avg}) \quad (16)$$

$$K_{avg} = \frac{K_{in} + K_{out}}{2} \quad (17)$$

where the inlet and outlet equilibrium constants are:

$$K_{in} = \prod \left( \frac{P_{i,in}}{P^0} \right)^{v_i} \quad (18)$$

$$K_{out} = \prod \left( \frac{P_{i,out}}{P^0} \right)^{v_i} \quad (19)$$

The electrochemical kinetic expression, required to compute the cell resistance, together with the numerical coefficients is reported elsewhere [7].

Obviously certain corrections have to be introduced to match the results of the intermediate-fidelity model to those of the reference model, at least at the nominal point. For the reformer, it is sufficient to include a single empirical approach to the thermochemical equilibrium: setting the temperature approach to a  $\Delta T$  value of 33 K, the model accurately matches the results. For the fuel cell, two additional empirical parameters were added to compensate for the effect of the coarse-grained discretisation: an offset tension ( $V_{offset}$ ) and an offset heat duty ( $Q_{offset}$ ). The values of these two empirical parameters at the nominal point were obtained by solving two additional equations simultaneously with the entire intermediate-fidelity system model:

$$V_{FC}^0 = \left[ V_{FC}^0 \right]_{rigorous} \quad (20)$$

$$\frac{T_{cat,in}^0 + T_{cat,out}^0}{2} = \left[ \frac{T_{cat,in}^0 + T_{cat,out}^0}{2} \right]_{rigorous} \quad (21)$$

where the right hand sides are the results of the system simulation using the rigorous model.

The choice of matching the two models by comparing the results for the entire system model and not just by comparing the intermediate-fidelity FC model with the rigorous one was suggested by the observation that this procedure minimizes the deviations. In fact when the match was obtained for the standalone FC, and the resulting tuned intermediate-fidelity FC model was plugged in the system model, some of the errors were amplified causing an unexpected deviation with respect to the rigorous system model.

The resulting numerical values for the two FC empirical parameters are small enough ( $V_{offset} = -0.18$  mV and  $Q_{offset} = 11.7$  kW) to make a good case for the chosen approach.

As shown in Table 3, when only the temperature-approach correction for the reformer is in place, there is just a moderate deviation in terms of electrical power output from the cell (after all  $V_{offset}$  is a really small number), but a few degrees of error in the cathodic temperatures are propagated to the reformer, influencing compositions and, finally, causing a large error in the prediction of the maximum solid temperature. When on the other hand all corrections are in place, the mass and energy balance around the fuel cell stacks match those of the detailed model quite closely.

### 3.2 Gas Turbine Sub-system Modelling

The recuperated, single-shaft Gas Turbine Sub-system model is based on concentrated-parameter models for all the units, as in the majority of the system studies reviewed (see section "Model Implementation and Performance"). For accurate pressure-driven modelling at part-load, the relationship between the rotation frequency, pressure and flow should be included, based on the characteristic curves of the turbine and compressor and the GTS control strategy.

The control of GTS is typically based on different approaches [8] that depend on the machine type and power range. For small, radial machines (such as automotive-derivatives in the net power range of tens of kW) it is based on changes to the rotation speed (i.e. the frequency) [9]. For larger, axial machines (such as aero-derivatives in the net power range of tens of MW) the frequency is constant and the flow/load is controlled by manipulating the geometry. The size of the GT unit which would be required for integration with the MCFC energy plant proposed in this study (net power in the range of 250 kW when in stand-alone operation) is between the typical ranges of automotive- and aero-derivatives. The lack of characteristic curves and of information on the control strategy would suggest simplifying the GTS model while retaining the key point, i.e. that the operating pressure and the fresh-air intake of the GTS are linked to the Turbine Inlet Temperature (TIT) by the overall GT characteristic. The simplified GTS part-load model is based on the following assumptions:

- geometries do not change and load control is achieved by changing the frequency;
- thermodynamic (isentropic) efficiencies will not change significantly;
- the operating point of the compressor should be kept clear of the stonewall and surge limits, and move along an optimal curve so that the dependence of the pressure ratio on the frequency is:

$$(\beta - 1) = (\beta^0 - 1) \cdot \left( \frac{n}{n^0} \right)^2 \quad (22)$$

- the corrected mass flows, defined by equation (23), are linear functions of the frequency of both the compressor and the turbine;

$$\dot{m}' = \dot{m} \cdot \frac{\sqrt{P_{in}}}{T_{in}} \quad (23)$$

- the turbine will operate at stonewall (incipient choked flow), so that the mass flow does not depend on the pressure ratio.

When this GTS modelling approach is considered, the TIT and the fresh-air flow to the GTS are calculated as a function of the operating pressure P (or, equivalently, of the pressure ratio) so that

the uncorrected mass flows of the compressor and turbine match the actual mass flows, and the frequency determines an operating point located on the optimal compressor curve.

#### 4. Model Matching and Extrapolation

We have described above the procedure used to match the results of the intermediate-fidelity system model to those of the rigorous one, with distributed models for the reformer and for the fuel cell stacks. This procedure is based on three parameters: the reformer temperature approach, the offset tension and the offset-heat duty of the fuel cell. The three empirical parameters can be considered analogous to the training coefficients of a neural network [10]; with the difference that they have some intuitive meaning and that the “training” takes place by solving a couple of simple algebraic equations that do not require elaborate regressions.

These parameters are empirical and have no extrapolability; the matching procedure should be repeated following any change in the process configuration, equipment size or any significant changes in the operating conditions. In other words, the relationship between the rigorous and the approximate model is tight, and the latter will give good results only if the operating point is close enough to the nominal point where the match (obtained for the same process configuration and equipment size) has been obtained.

In the sensitivity studies below, we will extrapolate the intermediate-fidelity model for a wide domain, without recalibrating the empirical parameters, and with the single provision that the offset-heat duty of the fuel cell ( $V_{\text{offset}}$ ) has been set to depend linearly on the cell current, based on the assumption that the offset will be reduced if the FCS load is reduced. It is therefore understood that the sensitivity studies have a qualitative nature and are not meant to predict the behaviour of the system quantitatively.

In the framework of an on-line application, the empirical parameters would be updated when the operating point changes significantly, by using mechanisms outside the scope of this work; either by executing the rigorous model at prescribed intervals or using the well-known techniques of adaptive control [11] or data reconciliation [12] to directly match the actual plant performance.

A possible improvement to extend the range of variation of the operating parameters would be to transfer the empirical parameters in the form of suitable maps (as a function of some key input parameters) obtained by repeatedly executing the matching procedure in the desired range.

#### 5. Example of Application

To reproduce the results of the reference 1 MW<sub>e</sub> hybrid MCFC-gas turbine energy plant we used the values for the model parameters shown in Table 4.

When the plant model has been set up for the rating calculation of all the units, with fixed heat-exchange areas, flow coefficients and stack parameters (stack arrangement, cell area, number of cells per stack) the available manipulated variables are:

- fuel cell current<sup>1</sup>;
- feed flow-rate of fuel to the FCS;
- cathodic purge ratio;
- split-ratio at GTS compressor outlet;
- operating pressure or, equivalently, feed flow-rate of fuel to the GT burner (R2) or Turbine Inlet Temperature (TIT);
- feed flow-rate of demineralised water.

It should be noted that the air flow to the GTS is a result of the set point for the GT subsystem, but the control algorithm can reduce the quota sent to the FCS by manipulating the compressor-outlet split-ratio.

The constraints that must be enforced to guarantee safe operation are:

- 1 The current is the natural variable to manipulate for two reasons:
  1. it is the actual manipulated variable in the industrial plant due to the design of the electrical subsystem;
  2. the current limits are physical whereas the limits for the voltage (especially the maximum voltage) vary as a function of the composition, temperature etc, making it more difficult to check *a priori* for unfeasible specifications.

- maximum temperature inside the stack < 963 K;
- steam-to-carbon ratio > 3.5;
- cathodic inlet temperature 873-893 K;
- anodic inlet temperature 843-893 K;
- O<sub>2</sub> molar fraction at the cathodic inlet > 8%;
- CO<sub>2</sub> molar fraction at the cathodic inlet > 5%;
- H<sub>2</sub> molar fraction at the anodic outlet > 6%;
- fuel-cell current density < 1550 A/m<sup>2</sup>;
- fuel cell stack pressure drops < 20 hPa;
- fuel utilisation in terms of CO + H<sub>2</sub> conversion < 75%;
- O<sub>2</sub> utilisation factor < 20%;
- CO<sub>2</sub> utilisation factor < 50%;
- maximum turbine-inlet temperature < 1273 K.

Initially the list of constraints seems overwhelming, since there are more constraints than MVs; it is not clear what the form and extension of the feasible operating region is, or if there is any degree of freedom left to seek some optimum.

To simplify the problem we exploit the fact that at the solution of an optimisation problem one or more constraints are at their limit; experience has shown that the first two in the list above (maximum temperature inside the stack and steam-to-carbon ratio) generally hit their bounds, while the anodic and cathodic inlet temperatures of the FC are generally in the middle of the range. So the problem has been transformed by turning these four inequality constraints into the following four algebraic equations:

- maximum temperature inside the stack (set at the bound) = 963 K;
- steam-to-carbon ratio (set at the bound) = 3.5;
- cathodic inlet temperature (set in the middle of the allowed range) = 883 K;
- anodic inlet temperature (set in the middle of the allowed range) = 868 K.

To conserve the balance between equations and unknowns, four of the previously user-specified MVs have to be used to solve the new equations, and our choice was to manipulate the fuel cell current, the flow of demineralised water, the cathodic purge-ratio and the compressor-outlet split-ratio. After this transformation we are left with the other operational constraints and the two following degrees of freedom:

- fuel-feed flow-rate to fuel cell;
- operating pressure.

We are now ready to study the sensitivities and the form of the feasible operating region, on the basis of a certain control objective.

Setting the objective function for the optimisation is outside the scope of this work, and would require an analysis of the fiscal and subsidy policies, environmental framework and deployment scenario. Possible optimisation objectives are maximising the electrical efficiency of the plant at partial electrical load or maximising the by-product electrical energy production at partial thermal duty.

In this application example we will assume that the objective of the servo problem is to produce a required, total net part-load electrical power output and that the objective of the optimisation is to maximise the plant electrical efficiency. During these studies the four former MVs (the fuel cell current, the demineralised-water flow, the cathodic purge-ratio and the compressor-outlet split-ratio) are continuously adjusted to satisfy the equations obtained from the four eliminated inequality constraints.

The fuel-feed flow-rate to the FCS is the natural parameter to change when it is desired to reduce the load below the nominal one; the effect at a constant pressure (equal to the nominal value of 3.6 bar) is shown in Figure 2, 3 and 4.

Within the part-load range of 30%-100% fuel-feed flow-rate to the FCS, none of the nine constraints is affected, but at the low end the O<sub>2</sub> utilisation factor is approaching the threshold value.

Figure 2 shows that indeed the fuel-feed flow-rate to the FCS can be used to lower the electrical power output, but the thermal (cogenerative) power output does not change as much. From Figure 3 it is apparent that the FCS efficiency is fairly constant over the range, with a slight maximum at 50% load, whereas the plant electrical efficiency decreases considerably at part load. This happens because of the increasing contribution of the GTS to the electric production (from 19% at the nominal point up to 44% at 30% power output); a GT of this size in standalone operation typically has an electrical efficiency of about 30-35% and as the contribution of the GTS becomes predominant the plant efficiency asymptotically approaches that of a standalone GT. The impact of the GTS increases at part-load in this constant-pressure scenario because as the cathode recycle flowrate decreases, the FCS exhaust (cathode offgas purge) from STACK1/2/3/4 to the GTS burner R2 is not bringing in enough sensible heat to drive the turbine T. The control algorithm reacts by increasing the GTS fuel flow rate to keep the flow through the machine constant while maintaining the pressure level; this in turn increases the turbine inlet temperature (Figure 4).

The effect of varying the operating pressure in the range 80-100% to control the load, with a constant fuel-feed flow-rate to the FCS equal to 50% of the nominal, is shown in Figure 5 and 6. In this case the electrical and thermal power output decrease simultaneously (Figure 5); the GTS contribution to the electric production decreases with decreasing pressure, and the plant electrical energy *increases* at part load.

The reason for this opposite trend is the decrease in low-efficiency power output from the GT obtained at the lower set pressure.

However, the system cannot function at pressures lower than about 3.1 bar (grey region) because the actual mass flows in the compressor and in the turbine cannot be matched; lowering the pressure also reduces the fresh-air intake and increases the oxygen utilisation factor towards its limit.

From these studies it is clear that an optimum strategy for controlling the load is obtained by simultaneously manipulating the pressure and the fuel-feed flow-rate to the FCS. Figure 7 presents a two-variable parametric plot when the fuel flow-rate to FCS and pressure are both in the vicinity of 50% of the nominal value; the grey area is unfeasible because the actual mass flows in the compressor and in the turbine can not be matched. The parametric plot shows that the maximum plant electrical efficiency at a constant net total electrical output is obtained at the operating point with the lowest pressure and the highest fuel flow-rate to the FCS.

Plotting Figure 7 was challenging; a center point was chosen, and the 2-D sensitivity was performed by spiralling around this point in progressively wider rounds. The spiralling path was chosen between several options for scanning the 2-D domain because it is more robust than other patterns; if the feasible domain has an irregular form, and given a feasible interior point, the spiralling path will stop when the convergence will fail, returning full results for the largest possible regular (rectangular) sub-domain.

The sensitivity studies performed using the modified model show that the behaviour of the system is very regular and linear over a wide MV range, thanks to the stabilising effect of the enforced constraints that either directly or indirectly lock the thermodynamic state and composition of the feeds to the reformer and FC, thereby effectively suppressing the main potential sources of non-linear behaviour.

Apart from the examples of applications discussed previously, it should be noted that the implementation of the new model simultaneously solves the flowsheets, even in the presence of complex, non-linear process specifications, thereby achieving stable convergence. Analytical derivatives are available, making it possible to accurately compute the sensitivities and the Relative Gain Array (RGA) matrix [13] for each operation point.

## 6. Model Implementation and Performance

System models for FC energy plants encountered in the literature are usually implemented using a commercial process-simulator as in [3] [14] and [15] or a commercial numerical-computing

environment as in [16], [17], [18] and [19]. Distributed-parameter models of the fuel cell stacks can be developed using commercial multiphysics tools [20], hand-written special purpose codes as in [3], [21] and [22], or within open-equation Process Simulators [23]. In particular in [3] the system model was implemented within a commercial process simulator, coupled with a hand-written special-purpose FORTRAN code for the MCFC stacks.

The steady-state process-model in this contribution has been implemented using the LIBPF 0.7 (LIBrary for Process Flowsheeting), a process flowsheeting and modelling tool being developed by the UNIGE-DICAT Group [24], arranged as a C++ library [25].

LIBPF natively supports hybrid-unit operations [26], steady-state and transient processes and, for the former both sequential modular and simultaneous resolutions of flowsheets with process specifications (feed-back) and the computation of analytical derivatives (sensitivities).

As the models for all the required components, reactions and unit operations were already available in the library and there is a high degree of code reuse, each tested system model required typing only about 500 lines of intuitive C++ code. The executable compiled from the C++ code is the calculation kernel which can be used to perform part-load and sensitivity studies through the user-friendly interface and without recompilation as long as the flowsheet connectivity does not change. The interaction between the calculation kernel and the user interface takes place via interprocess communication and the standard object-oriented database interface ODBC [27]; the underlying relational database makes the instantiated objects persistent and eases the access to the results using third-party applications or from another workstation on the network.

There are two requirements of a first-principle steady-state process model to form the core model of an on-line application that are related to performance: being lean, i.e. lightweight, and efficient, i.e. fast.

The space occupied by the special-purpose executable produced with the LIBPF library is very limited: the calculation-kernel executable is less than 3 MB and only depends on the operating system and compiler-runtime dynamic-link libraries. The memory at run-time is dynamically allocated and the maximum memory footprint is less than 15 MB. The Valgrind tool [28] was used to ensure that the code was free of memory leaks.

The programme execution on a modern workstation takes a few tens of seconds for the first-time sequential resolution and initialisation, while a simultaneous evaluation of the residuals and their derivatives takes less than 200 ms. These figures have to be compared with minutes when running a rigorous model. Furthermore, the scaling performance of the parallel version of the tool has demonstrated speed-ups of about 50% of the theoretical on multi-core workstations [29].

## 7. Conclusions

The application of reconciliation, identification or advanced-control techniques to hybrid Molten Carbonate Fuel Cell–Gas Turbine energy plants for Combined Heat and Power is very interesting: the expected benefits lie in increased safety, flexibility and optimum operation.

With the objective of complying with the requirements of a process model for on-line applications, we have developed an intermediate-fidelity steady-state system model of the energy plant together with a method to tune the approximate model to match the results of more detailed models in a certain operating point, based on fitting just three empirical parameters.

Since the high number of operating constraints on temperatures, compositions etc. made it difficult to get an idea of the form of the domain of feasible operation, the problem was further simplified. The constraints were sorted based on the criterion of prioritizing those that most often were found in practice to be limiting, and the most significant inequality constraints were transformed into equations that can be solved simultaneously with the model.

The final model has only two degrees of freedom left (the pressure and the fuel fed to the MCFC unit) and satisfies the other constraints automatically over a wide range of the manipulated variables.

The 2-D analysis of the sensitivities yields a map of the Key Performance Parameters (total net electric output and plant electrical efficiency) as a function of these two degrees of freedom. This map is an intuitive, qualitative tool to identify the optimum operating conditions; from the map it is

also clear that to overcome the limits in the operating flexibility of the plant the control strategy of the GTS should be improved.

The implementation, based on the LIBPF library, employs a simultaneous solution strategy and efficiently computes analytical derivatives and the RGA matrix, making the tool immediately suitable for integration in an on-line application.

Planned future developments will focus on improving the model by implementing the empirical parameter maps discussed above, extending this approach to other fuel cell systems such as Solid Oxide Fuel Cells (SOFCs) and proton-conducting SOFCs, and finally move on to a dynamic model of the process, as it is possible to solve the Differential Algebraic Equations associated with a dynamic model with the LIBPF tool used. The dynamic model of the fuel cell can be developed by including both the slow thermal inertia [30] and the fast-capacitance effects [31].

## Acknowledgements

The authors wish to thank Paolo Costa of DICAT (University of Genova) for support and advice.

## References

1. European Hydrogen and Fuel Cell Technology Platform (HFP) Implementation Plan – Status 2006, endorsed by the HFP Advisory Council on January 19, 2007.
2. Siemens Power Generation press release, October 31, 2005.
3. Marra D, Bosio B. Process analysis of 1MW MCFC plant. *Int. J. Hydrogen Energy* 2007; 32: 809-818.
4. Daubert T E, Danner R P, Sibul H M, Stebbins C C editors, DIPPR Data Compilation of Pure Compound Properties - AIChE DIPPR - Project 801. Taylor and Francis: Bristol, PA 1996.
5. Aly F A and Lloyd L L, Self-consistent equations for calculating the ideal gas heat capacity, enthalpy, and entropy, *Fluid Phase Equilibria* vol. 6 Pages 169-179
6. Lanzafame R and Messina M, A New Method for the Calculation of Gases Enthalpy, IECEC 2000 (Intersociety Energy Conversion Engineering Conference), AIAA-00-2851, Vol. 1, pp. 318-328
7. Arato E, Bosio B, Costa P, Parodi F, Preliminary experimental and theoretical analysis of limit performance of molten carbonate fuel cells, *Journal of Power Sources*, 102, 2001, pp. 74-81
8. Won Song T, Lak Sohn J, Seop Kim T and Tack Ro S. Performance characteristics of a MW-class SOFC/GT hybrid system based on a commercially available gas turbine. *Journal of Power Sources* 2006; 158(1): 361-367.
9. Colombo LPM., Armanasco F and Perego O. Experimentation on a cogenerative system based on a microturbine. *Applied Thermal Engineering* 2007; 27(4): 705-711.
10. Choi TI, Lee KY, Junker ST and Ghezal-Ayagh H. Neural Network Supervisor for Hybrid Fuel Cell/Gas Turbine Power Plants. *Power Engineering Society General Meeting*, 2007; 1 – 8 Digital Object Identifier 10.1109/PES.2007.385503.
11. Mishkin, E. and Braun LJ. *Adaptive Control Systems*. New York NY: McGraw Hill Book Co. Inc., 1961.
12. Schladt M and Hu B, Soft sensors based on nonlinear steady-state data reconciliation in the process industry. *Chemical Engineering and Processing: Process Intensification* 2007; 46(11): 1107-1115.
13. Bristol EH, On a new measure of interaction for multivariable process control. *IEEE Transactions on Automatic Control* 1966; 11(1): 133- 134.
14. Orecchini F, Bocci E, Di Carlo A, MCFC and microturbine power plant simulation. *Journal of Power Sources* 2006; 160(2): 835-841.
15. Freni S, and Cavallaro S, Catalytic partial oxidation of methane in a molten carbonate fuel cell, *International J Hydrogen Energy* 1999; 24 (1): 75-82
16. Lukas MD and Lee KY. Model-Based Analysis for the control of Molten Carbonate Fuel Cell Systems. *Fuel Cells*; 5(1): 115-125.
17. Roberts RA, Brouwer J, Liese E and Gemmen RS. Dynamic Simulation of Carbonate Fuel Cell-Gas Turbine Hybrid Systems. *J of Engineering for Gas Turbines and Power* 2006;

- 128(2): 294-301.
18. Korsgaard A R, Nielsen M P and Kær S K, Part one: A novel model of HTPEM-based micro-combined heat and power fuel cell system, *International Journal of Hydrogen Energy* Volume 33, Issue 7, April 2008, Pages 1909-1920
  19. Colpan C O, Dincer I and Hamdullahpur F, Thermodynamic modeling of direct internal reforming solid oxide fuel cells operating with syngas, *International J Hydrogen Energy* 2007; 32 (7): 787-795
  20. Subramanian N, Haran BS, White RE, and Popov BN, Full Cell Mathematical Model of a MCFC. *J. Electrochem. Soc.*; 2003; 150(10): A1360-A1367.
  21. Bosio B, Costamagna P, Parodi F, Modeling and Experimentation of Molten Carbonate Fuel Cell Reactors in a Scale-Up Process. *Chemical Engineering Science* 1999(54): 2907-2916.
  22. Jang J H, Yan W M, Li H L, Tsai W C, Three-dimensional numerical study on cell performance and transport phenomena of PEM fuel cells with conventional flowfields, *International J Hydrogen Energy* 2008; 33(1): 156-164
  23. Heidebrecht P and Sundmacher K. Molten carbonate fuel cell (MCFC) with internal reforming: model-based analysis of cell dynamics. *Chemical Engineering Science* 2003; 58, (3-6): 1029-1036.
  24. Greppi P. LIBPF: a Library for Process Flowsheeting in C++. *Proceeding of the International Mediterranean Modelling Multiconference* 2006: 435-440.
  25. ISO 1998, Programming Language C++, ISO/IEC 14882:1998
  26. Greppi P, Bosio B, Arato E. Object-oriented modelling applied to hybrid unit operations. *Chemical Engineering Transactions*, 2007; 11 *Proceedings of 8th International Conference on Chemical and Process Engineering*:113-118.
  27. Microsoft Corporation, 2004 ODBC Programmer's Reference.
  28. Nethercote N and Seward J, Valgrind: A Framework for Heavyweight Dynamic Binary Instrumentation. *Proceedings of ACM SIGPLAN 2007 Conference on Programming Language Design and Implementation*, San Diego, California, USA.
  29. Greppi P, Tearing for Parallelization and Control of Sparsity in Process Flowsheeting. in preparation for ESCAPE-18, June 2008 Lyon – France.
  30. Bosio B, Arato E, Molten Carbonate Fuel Cell System Simulation Tools. In: Zhang XW, editor. *Advances in Fuel Cells*, Trivandrum: Research Signpost, ISBN 81-308-0026-8, 2005.
  31. Zenith F, Skogestad S. Control of fuel cell power output. *Journal of Process Control* 2007; 17: 333–347.

## Figure Captions



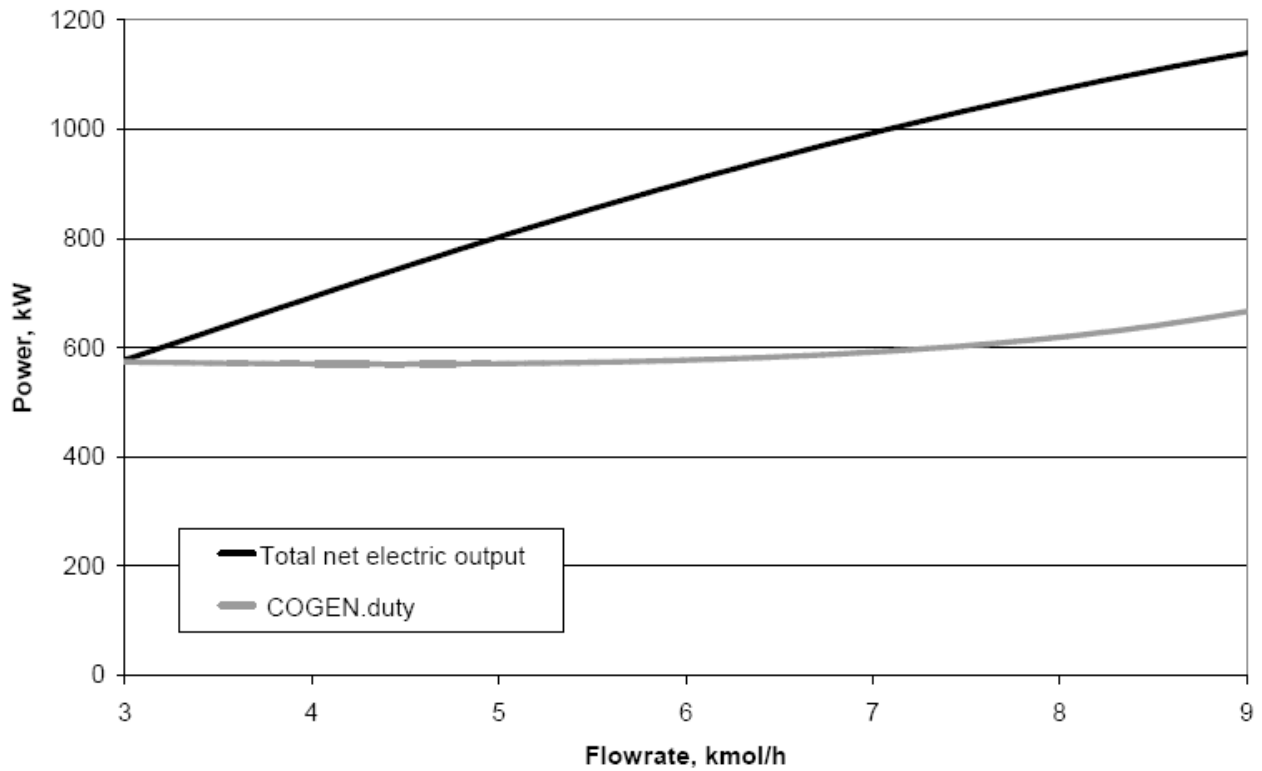


Figure 2 – Effect of the feed flow-rate of fuel to the FCS on the power output at the nominal operating pressure.

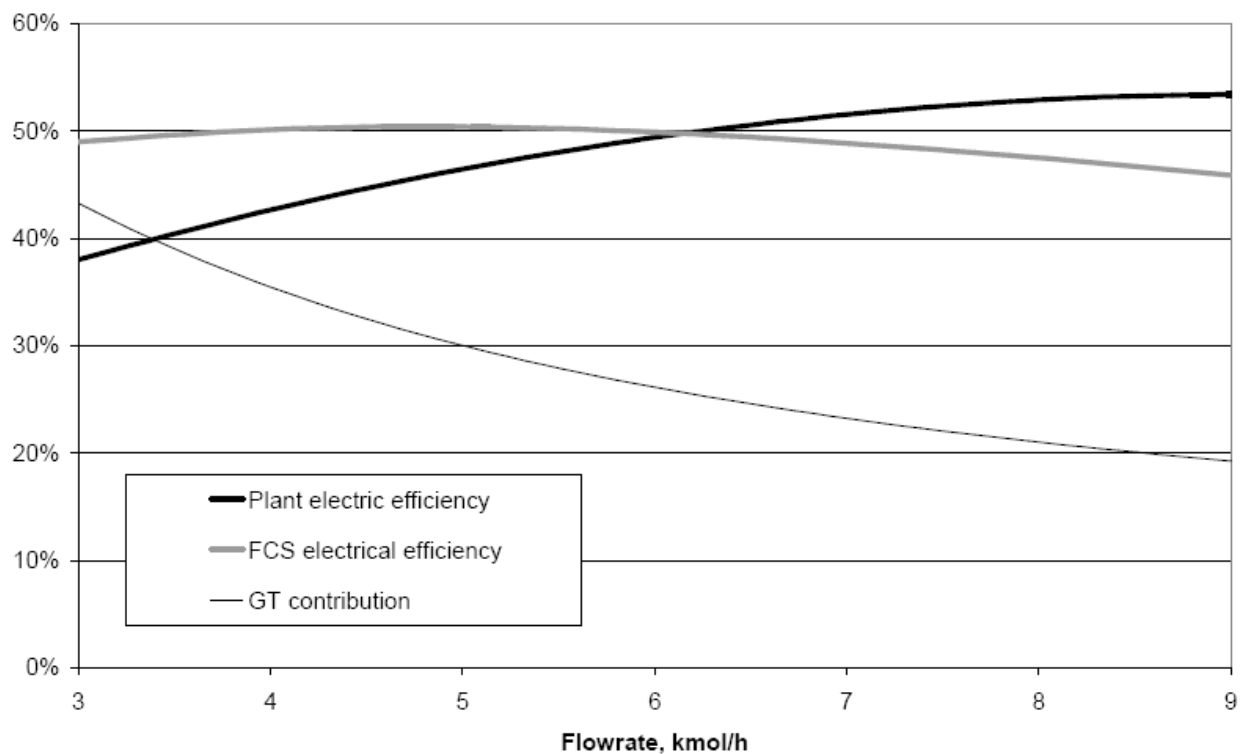


Figure 3 – Effect of the feed flow-rate of fuel to the FCS on the key operating parameters at the nominal operating pressure.



Figure 4 – Effect of the feed flow-rate of fuel to the FCS on the oxygen utilisation factor and the turbine inlet temperature at the nominal operating pressure.

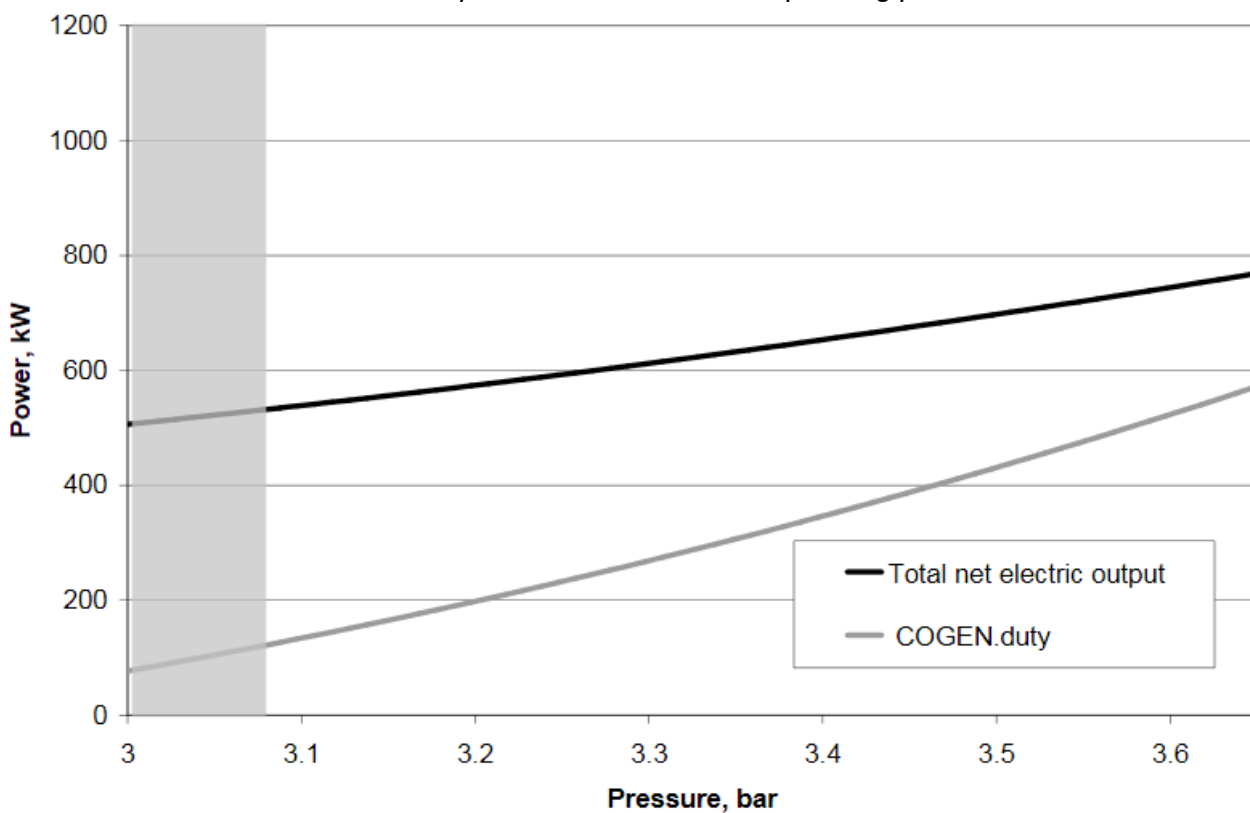


Figure 5 – Effect of the operating pressure on the power output at 50% fuel-feed flow-rate to the FCS.

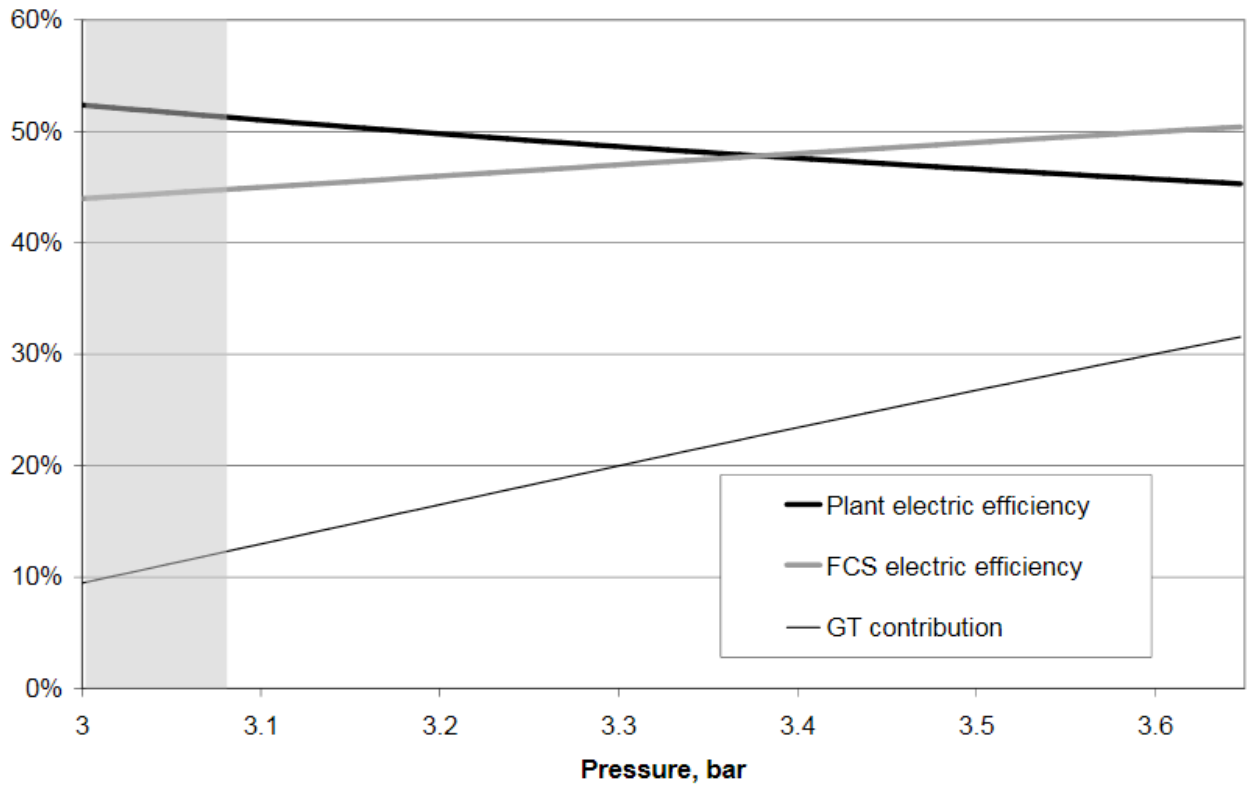


Figure 6 – Effect of the operating pressure on the key operating parameters at 50% fuel-feed flow-rate to the FCS.

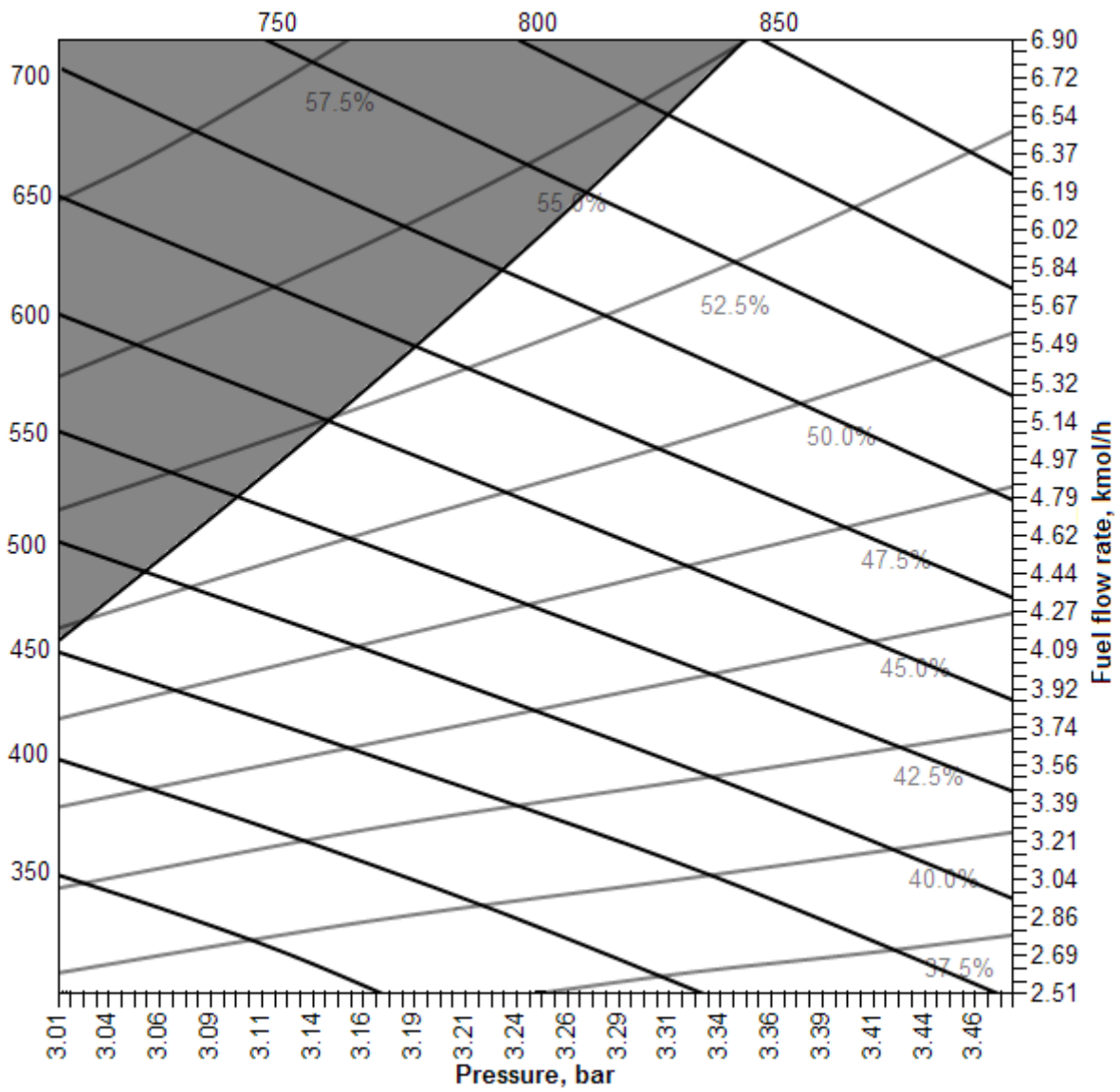


Figure 7 – Effect of the operating pressure and feed flow-rate of fuel to the FCS; constant total net electric output in black (W), constant plant electrical efficiency curves in grey.

## Tables

Fuel		
$\dot{n}$	0.002708729	kmol/s
T	296	K
P	3.6	bar
Air		
$\dot{n}$	0.057769364	kmol/s
T	296	K
P	1.01325	bar
Fuel cell		
J	1547.1	A/m <sup>2</sup>
$W_{el}$	1007.02	kW
GTS		
$W_{me, T}$	217.6	kW
Net power production		
$W_{el,net}$	1160	kW
$W_{th,net}$	687.5	kW

Table 1 – Summary of results for the reference 1 MW plant

Component	H <sub>2</sub> O	N <sub>2</sub>	O <sub>2</sub>	CH <sub>4</sub>	CO	CO <sub>2</sub>	H <sub>2</sub>
$\Delta H^0$ , kJ/kmol	-241814	0	0	-74520	-110530	-393510	0
$\Delta G^0$ , kJ/kmol	-228590	0	0	-50490	-137150	-394370	0

Table 2 - Pure components enthalpy and Gibbs free energy at the reference state

	Maximum Absolute Error	
	With reformer T approach correction only	With all corrections in place
$W_{el,FCS}$ , W	1300	0
$T_{an,avg}$ , K	9.4	4
$T_{cat,avg}$ , K	5.4	0.3
$T_{s,max}$ , K	25	4
$x_{an}$	0.4%	0.08%
$x_{cat}$	1 ppm	1 ppm

Table 3 – Comparison of results around the MCFC stacks

Ambient temperature	296	K
FC.w	0.1195	m
FC.I	0.595	m

FC.N	300	
FC. $\Delta P_{an}$	4	hPa
FC. $\Delta P_{ca}$	21	hPa
FC.U	500	W/m <sup>2</sup> /K
REFORMER. $\Delta P_{ho}^{nom}$	28.0	hPa
RECUPERATOR. $\Delta P_{ho}^{nom}$	50.0	hPa
RECUPERATOR. $\Delta P_{co}^{nom}$	10.0	hPa
R1. $\Delta P$	40.0	hPa
R2. $\Delta P$	150	hPa
REFORMER. $k_{ho}$	93.6	kg/m <sup>7</sup>
RECUPERATOR. $k_{ho}$	265.3	kg/m <sup>7</sup>
RECUPERATOR. $k_{co}$	1205320	kg/m <sup>7</sup>
BLOWER. $\theta$	70	%
BLOWER. $\eta_{el}$	100	%
BLOWER. $\eta_{me}$	100	%
C. $\theta$	75	%
C. $\eta_{el}$	100	%
C. $\eta_{me}$	100	%
T. $\theta$	85	%
T. $\eta_{el}$	100	%
T. $\eta_{me}$	100	%
COGEN. $T_{ho,out}$	363	K
REFORMER.(U·A)	5188.57	W/K
REGHEX.(U·A)	206.108	W/K
SPS.(U·A)	1965.02	W/K

Table 4 – Numerical values of the model parameters used